AECL-12018

RAMAN SPECTROSCOPY FOR IN-SITU CHARACTERISATION OF STEAM GENERATOR DEPOSITS

P.A. Rochefort, D.A. Guzonas, and C.W. Turner

AECL
Chalk River Laboratories
Chalk River, Ontario
Canada, K0J 1J0

INTRODUCTION

Fouling of the secondary-side of nuclear steam generators (SG) by corrosion products and other impurities that have been transported into the SG with the feedwater is a serious problem. The build-up of deposits on the SG tubes can lower the rate of heat transfer[1,2], and act as sites for the concentration of impurities leading to localised corrosion of the underlying substrate. When fouling is severe, the deposits must be removed by chemical and/or mechanical cleaning techniques. Information on the composition of the deposits is then required for the development of optimal cleaning conditions and procedures. The composition of the deposits also provides information on the chemistry conditions within the SG and the feedtrain[3,4].

Although samples of deposit can be removed from the steam generator for ex-situ characterisation, for example, after waterlancing, the quantity of deposit available is often limited, and the exact origin of the recovered deposit is not always known. Samples removed may also undergo chemical or physical surface alteration upon exposure to the atmosphere. An in-situ inspection technique capable of identifying the chemical composition of the compounds present in a deposit, and of giving a semi-quantitative measurement of their concentrations, would therefore provide valuable information.

Recent advances in filter and detector technologies coupled with the use of fibre optics make Raman spectroscopy a useful remote characterisation method of materials by vibrational spectroscopy. Fibre optics are used to transmit laser energy to the inspection area and scattered light back to the spectrometer. Remote Raman spectroscopy using fibre-optics is now being used in plant environments to characterise a variety of materials[5] . A

recent review of the application of fibre optics for Raman spectroscopy can be found in a recent paper by Lewis and Griffiths[6].

We have constructed several fibre optic probes capable of measuring Raman spectra of secondary-side deposits, in an on-going program to develop and demonstrate fibre-optic Raman spectroscopy for in-situ deposit analysis.

EXPERIMENTAL

In Raman spectroscopy, a sample is irradiated by a monochromatic light source (typically from a laser) and the scattered light is collected and analysed by spectrophotometer. Most of the incident light is elastically (Rayleigh) scattered without any frequency change. However, a small portion of the light, typically 1 photon in 10^6, is inelastically (Raman) scattered by the material, the frequency shift of the light (normally measured in units of inverse centimetres, cm^{-1}) is proportional to the transition energy between vibrational energy levels of the molecules or crystal structures in the sample. The frequency, width, and relative intensities of the spectral peaks can be used to determine the identity and quantity of the compounds in the sample.

There are two major problems in obtaining Raman spectra of solid metal oxide samples using fibre optics. The first is preventing the Raleigh scattered light in the total scattered signal from entering the spectrometer so that the detection system is not swamped. The second is the removal of the silica (or glass) Raman spectra produced by the fibre as it transmits the laser energy to the sample and the Rayleigh scattered light from the inspection area. The principal bands of silica Raman spectrum occurs between about 100 to 600 cm^{-1}, the same region as the bands of most of the oxides found in SG deposits.

A demonstration Raman illumination and collection optical system that addresses these problems has been fabricated (see Figure 1). At its core, a holographic notch filter (Kaiser Optical HSPF-647-1.0) is used both as a reflective optical component for the incident laser light and as a notch filter for the Raman scattered light. Holographic notch filters reflect almost 100% of the design wavelength while transmitting more than 80 % of light with longer or shorter wavelength. Typical filter rejection bandwidth around the central wavelength is 600 cm^{-1}.

The optical assembly is approximately 200 mm long and 40 mm in diameter. The input laser beam, steered directly from the laser as shown in the figure, or carried by an optical fibre, enters near the base of the assembly at right angles to the vertical optical axis. The beam is reflected up by an adjustable mirror onto the centre of the notch filter, which is set at 5 degrees off-normal to the optical axis. The position and angle of the mirror is adjusted so that the laser beam is reflected by the filter down the centre of the optical axis through a 0.4 numerical aperture (NA) long working distance microscope objective (Leitz H32X/0.60). When the laser light is transmitted by an optical fibre, the silica induced Raman spectrum is removed from the laser beam because the frequency shifted light is transmitted through the holographic filter.

A sample is placed at or near the focal point of the beam, and scattered light from the sample is collected and collimated by the objective and directed back up to the notch filter. Raleigh scattered light is reflected by the notch filter, whereas wavelength-shifted light is transmitted through the filter. The filtered light is concentrated by a condenser lens onto the end of a fibre optic bundle and transmitted to the spectrometer. The use of a single objective to both focus the laser beam and collect the scattered light significantly reduces

the alignment complexity as compared to a two lens optical arrangement, one to focus the laser beam and one to collect the scattered light.

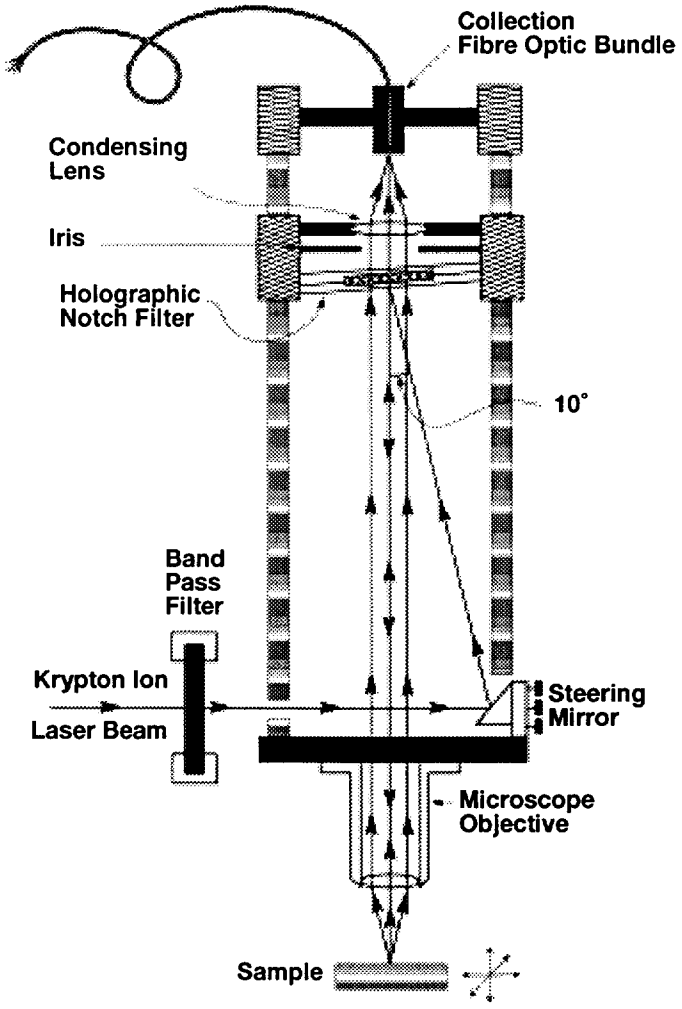

Figure 1: Schematic of the fibre optic Raman collection system

The fibre optic bundle consists of 7 step-index multi-mode fibres having 200 μm pure silica cores. The bundle is 3 meters long and terminated at each end with modified standard fibre optic couplers. At the collection end, the fibres are arranged in six-around-one close-packed geometry while at the other end, used as the source for the spectrometer the fibres are arranged in a close packed line. The output of the fibre bundle is focused on the spectrometer slits. Both ends are polished flat.

Raman spectra were measured using a SPEX 1000M single monochromator with a charge-coupled device (CCD) detection system. The detector integration times and the number of signal-averaged acquisitions were optimised to give the best signal-to-noise ratio for each sample. Typical values were 10 to 40 second integration times and 4 to 16 acquisitions. The 647.1 nm line from a Krypton ion laser was used for excitation; laser plasma lines were removed using a bandpass filter (10 nm bandwidth) centred at the laser frequency. The laser power incident on the samples was approximately 30 mW.

Raman spectra were acquired over the range 200-1600 cm^{-1} in several overlapping windows which were then spliced together. Data manipulations such as baseline correction and spectral splicing were carried out using a spectrum analysis software package (GRAMS/386, Galactic Industries Inc.)

RESULTS

The Raman spectra of the various iron oxide phases expected in these deposits have been well documented in the literature[7,8,9]. The Raman spectra of the three most common iron containing phases found in CANDU (CANada Deuterium Uranium) SG deposits, magnetite, hematite and nickel ferrite, are shown in Figure 2 over the spectral range of 150 to 840 cm^{-1}.

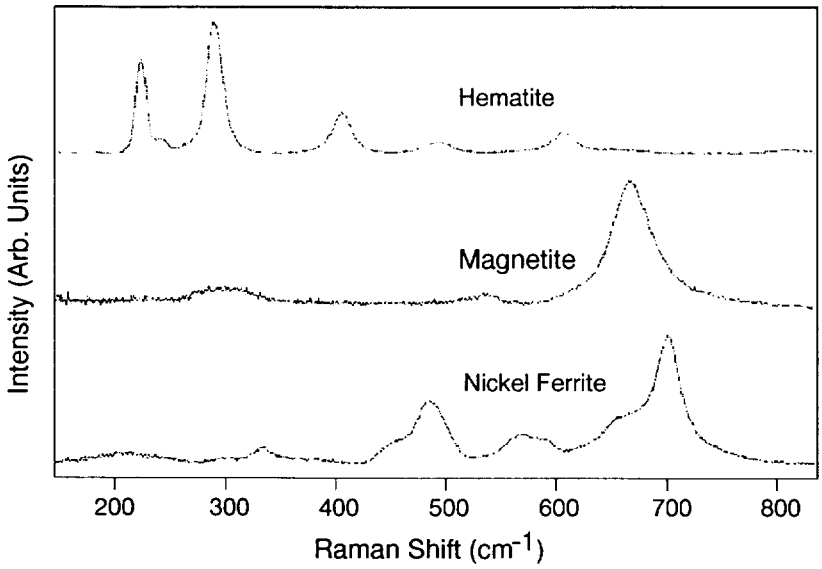

Figure 2: The Raman spectra of the three most common iron oxide phases found in the CANDU deposits.

In mixtures of particles of strongly absorbing oxides such as magnetite, Raman band intensities do not vary linearly with the concentration of the oxide phases present due to scattering and light absorption by the particles. Quantification of the composition of such a mixture therefore requires the use of suitable calibration mixtures. Calibration mixtures of magnetite and hematite as well as magnetite and nickel ferrite were prepared by mechanically mixing the pure powders to produce a homogeneous mixture. Raman band intensities were then plotted against concentration, and an empirical calibration curve fit to the data.

As the concentration of magnetite in the deposit samples increased, it became increasingly more difficult to obtain a Raman spectrum as a result of the strong absorption of the laser light by magnetite. Sample degradation often occurred unless care was taken to optimise the focus of the laser. This degradation was usually indicated by the appearance of strong hematite bands in the Raman spectrum after short exposure of the sample to the laser, a result of oxidation of the surface of the magnetite to hematite. A red coloured damage zone could often be observed visually at the spot where the laser beam had struck the sample. These factors made it much easier to obtain Raman spectra from the samples which contained low concentrations of magnetite. Recognisable spectra from samples containing large amounts of nickel ferrite or hematite could be obtained with an integration time of about one second, while samples consisting mainly of magnetite required integration times of about 10 seconds.

The three samples investigated had been removed from steam generators by waterlancing. Two were in the form of loose powders, and the third was a millimetre-sized flake. The samples had previously been examined by X-ray diffraction (XRD), and the

first sample had been extensively characterised by Mossbauer spectroscopy and other analytical techniques.

Raman spectra of the three secondary-side deposits are shown in Figure 3, over the 200-800 cm^{-1} spectral region. The spectrum in Figure 3a contains a strong band envelope in the 640-710 cm^{-1} region characteristic of nickel ferrite (NF). The strongest magnetite band is also observed, at approximately 665 cm^{-1}, and is marked with an M in the figure. Although the nickel ferrite and magnetite bands overlap in this spectral region, the intensities of the magnetite and nickel ferrite peaks under the band contour can be used to estimate the relative amounts of magnetite and nickel ferrite. It was estimated that 65% ±5% of the total spinel phase present was nickel ferrite and 35% ±5% was magnetite. For comparison, the composition determined by X-ray and Inductively Coupled Plasma-Atomic Emmission Spectroscopy (ICP-AES) indicated 15% magnetite and 85% nickel ferrite, while Mossbauer spectroscopy suggested the composition is 44% magnetite and 47 % nickel ferrite, with the remainder being zinc ferrite. The Raman results are therefore intermediate between these two analyses.

The Raman spectrum of the deposit in Figure 3b clearly shows the presence of both hematite and magnetite. Based on reference mixtures of these two materials, the ratio of magnetite to hematite is estimated to be 5:2. Analysis by XRD gave an estimate of the magnetite to hematite ratio of 3:1, in good agreement with the Raman data. The Raman spectrum in Figure 3c, contains a band due to magnetite at 684 cm^{-1}, and also bands at 490, 634 cm^{-1}.

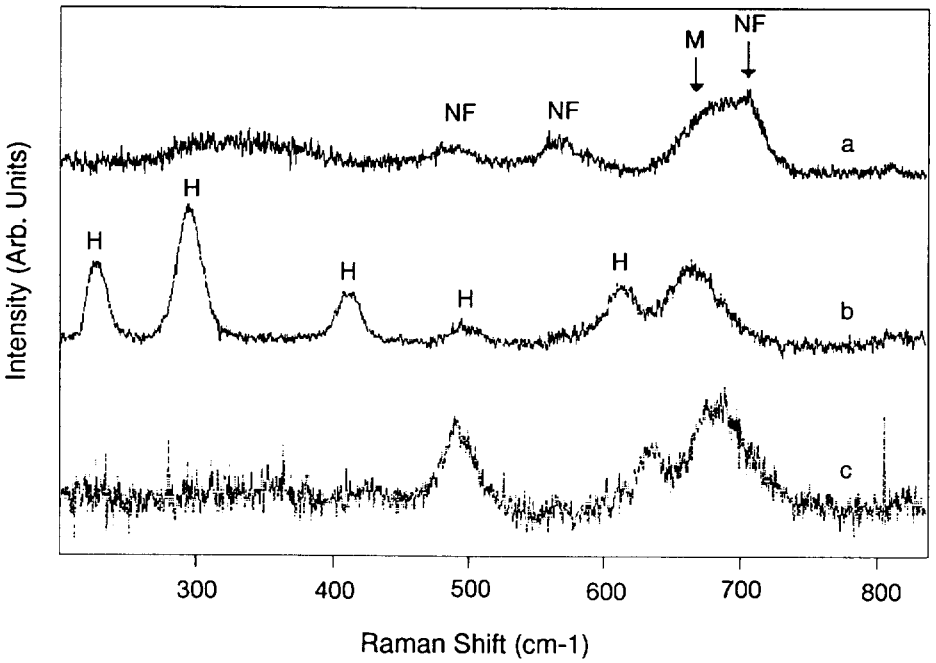

Figure 3: Representative Raman spectra of waterlanced CANDU secondary-side deposits

CONCLUSIONS

The work presented here demonstrates that good quality Raman spectra of steam generator secondary-side deposits can readily be obtained using a fibre optic based Raman spectrometer. The major chemical phases, other than metallic copper, can be readily

identified, and a semi-quantitative estimate of the composition can be made, as verified by comparison with deposit analyses performed using other techniques. This work suggests that in-situ characterisation of secondary-side deposits using fibre-optic Raman spectroscopy is feasible.

Laser-induced decomposition was noted for samples containing large concentration of magnetite. The decomposition usually resulted in the formation of hematite, and an increase in the intensity of hematite bands with time was a good indicator for decomposition. This decomposition could be minimised by working at low laser powers and using a slightly defocused laser. The presence of water with the samples did not adversely affect the spectra, but rather improved the quality of the spectra obtained from the powder samples by minimising laser-induced decomposition.

The spectra obtained from the flake samples clearly illustrate the heterogeneous nature of these deposits. Several Raman bands were found which could not be definitively assigned to a particular chemical species.

ACKNOWLEDGEMENTS

Funding for this work was provided by the CANDU Owners Group (COG), Technical Committee 19. The authors would like to thank COG for permission to publish this work. The authors would like to thank Bruce Nuclear Generating Station, Pickering Nuclear Generating Station, and Gentilly-2 Nuclear Generating Station for providing the samples studied in this work. The authors would also like to acknowledge J. Semmler for providing the XRD, ICP-AES, and Mossbauer analytical data for the sludge samples.

REFERENCES

1. T.F. Habib, P.A. Sherburne, J.F. Dunne, and C.L. Williams, Degradation in Ginna steam generator tube heat transfer due to secondary-side fouling, in: *Steam Generator Sludge Deposition in Recirculating and Once Through Steam Generator Upper Bundle and Support Plates*, NE-Vol. 8, ASME, 1992.
2. C.W. Turner and S.J. Klimas. Thermal resistance of boiler tube deposits at steam generator operating conditions, in: *Proceedings: Sludge Management Workshop*, May 10-12, 1994, Norfolk. Virginia. EPRI Report TR-104212.
3. W.A. Byers, P.J. Kuchirka, M. Rootham, and A.J. Baum. Can traces from the past predict the future?, in: *Electric Power Research Institute Surface Chemistry Workshop*, August 22-23, 1996, Myrtle Beach S.C.
4. C.W. Turner and K. Shamsuzzaman. The role of copper in sludge consolidation, in: *Proceedings: Sludge Management Workshop,* May 10-12, 1994, Norfolk. Virginia. EPRI Report TR-104212.
5. J. Andrews. Raman spectroscopy moves on-line, *Spectroscopy Europe*, 7, 8, (1995).
6. I.R Lewis, P.R. Griffiths, Raman spectroscopy with fiber-optic sampling, *Appl. Spectrosc.* 50, 12A (1996).
7. J. Gui, T.M. Devine. In-situ vibrational spectra of the passive film on iron in buffered borate solution, *Corrosion Science*, 32, 1105 (1991).
8. J. Dunwald and A. Otto. An investigation of phase transitions in rust layers using Raman spectroscopy, *Corrosion Science*, 29,1167 (1989).
9. R.J. Thibeau, C.W. Brown, and R.H. Heidesbach. Raman spectra of possible corrosion products of iron, *Appl. Spectrosc.*, 32, 532 (1978).